Realistic Autofarming Closed-Loop Tractor Control over Irregular Paths Using Kinematic GPS

Thomas Bell, Michael O'Connor, V. K. Jones, Andrew Rekow, Gabriel Elkaim and Bradford Parkinson

(Stanford University, CA, USA)

High-precision 'autofarming' makes possible farming techniques previously impractical using metre-level Differential GPS-based control systems: techniques such as tape irrigation, the elimination of guess rows, and precise contour farming. A Carrier-Phase Differential GPS positioning and attitude system with centimetre-level and 0·1° accuracy was installed in a large farm tractor. Four types of trajectories (lines, arcs, spirals, and curves) were identified as basic building blocks necessary to generate a 'global' trajectory for a realistic autofarming path. Information about each trajectory type was translated into reference state specifications that a linear controller used to control the tractor over velocities between 0·7 and 2·8 m/s to within approximately 6 cm (1 σ) without implement and 10 cm (1 σ) with implement on sloped terrain using a previously developed tractor model. These results are a significant step towards a realistic autofarming system because they not only demonstrate accurate control over various realistic operating speeds but over different types of trajectories necessary for a commercial system.

1. INTRODUCTION. At Stanford University, research into centimetre-level automatic tractor control is an outgrowth of previous positioning research involving aircraft.[1–3] Because a farm typically has good satellite visibility, agriculture was chosen to research practical land-based applications of Carrier-Phase Differential GPS (CDGPS). At Stanford, we have coined the term 'autofarming' to include not only precise positioning and control of agricultural vehicles, but also other technologies which could be integrated into such a precise control system.

There are three components to high-precision autofarming: measuring the tractor location to within centimetres; determining the desired tractor trajectory satisfying some user-defined requirement (such as spraying a field with minimum overlap); and actually controlling the tractor to move along the reference trajectory. The first component has been met through CDGPS. The second component involves robot motion planning. This paper focuses on the third component: a control system that steers the tractor along basic trajectory types including lines, arcs, spirals, and curves. The majority of realistic trajectories would incorporate a combination of these four 'building blocks'. Arc and spiral paths are often encountered in circular irrigation patterns. Curved trajectories could come from field boundaries (such as a stream) or from contour farming.

This paper outlines a tractor model, explains how to translate the four types of trajectories into tracking reference states for the tractor, and shows how to use those reference states to control the tractor accurately.

2. LINEARISED TRACTOR MODEL. Development of the tractor model has been detailed in previous research.[4] As shown in Fig. 1, d is the distance from

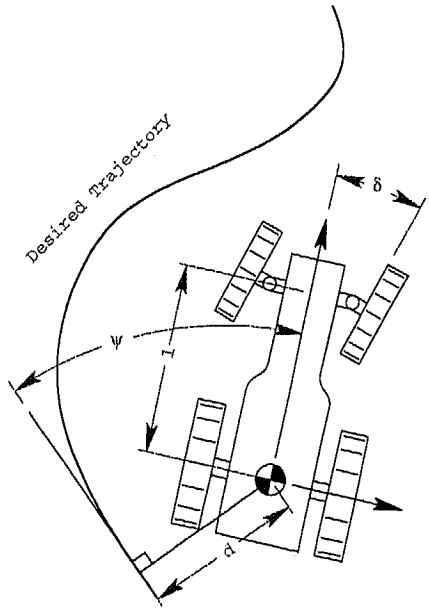

Fig. 1. Variable definitions

the closest point along the reference trajectory, ψ is the yaw angle of the tractor relative to the trajectory at that point, δ is the front wheel angle relative to the centreline of the tractor (i.e. body coordinate frame), and ℓ is the distance from the front wheels to the centre of the rear axle (assumed to be the pivot point). Two lag states, one in yaw rate and the other in steer angle rate, were added to improve the model based on experimental observations. The parameters τ_ψ and τ_v shown in equations (1) and (2) were identified from experimental data. The non-linear equations of motion can be written as

$$\ddot{\psi}_a = \frac{1}{\tau_\psi}(\dot{\psi}_c - \dot{\psi}_a) \tag{1}$$

$$\ddot{\delta}_a = \frac{1}{\tau_u}(u_c - \dot{\delta}_a) \tag{2}$$

$$\dot{d} = V \sin(\psi_a) \tag{3}$$

where the subscript a denotes 'actual' and c denotes 'commanded'.

The parameter V is the forward speed of the tractor. Yaw rate and steer angle are related by

$$\dot{\psi} = \frac{V}{\ell}\tan(\delta). \tag{4}$$

For control purposes, an integral state on the lateral error (d) was added to offset modelling errors. Yaw angle, steer angle, and lateral deviation were observable. The linearised state equations become

$$x \equiv [\psi_a \; \dot{\psi}_a \; \delta_a \; \dot{\delta}_a \; d \; \int d]^T$$

$$\dot{x} = \begin{bmatrix} 0 & 1 & 0 & 0 & 0 & 0 \\ 0 & -\frac{1}{\tau_\psi} & \frac{V}{\ell\tau_\psi} & 0 & 0 & 0 \\ 0 & 0 & 0 & 1 & 0 & 0 \\ 0 & 0 & 0 & -\frac{1}{\tau_u} & 0 & 0 \\ V & 0 & 0 & 0 & 0 & 0 \\ 0 & 0 & 0 & 0 & 1 & 0 \end{bmatrix} x + \begin{bmatrix} 0 \\ 0 \\ 0 \\ \frac{1}{\tau_u} \\ 0 \\ 0 \end{bmatrix} u_c$$

$$y = \begin{bmatrix} 1 & 0 & 0 & 0 & 0 & 0 \\ 0 & 0 & 1 & 0 & 0 & 0 \\ 0 & 0 & 0 & 0 & 1 & 0 \end{bmatrix} x.$$

3. SPECIFICATION OF TRAJECTORIES AND GENERATION OF REFERENCE STATES. There were five reference states to be specified for the tractor to follow a trajectory: yaw angle, yaw rate, steer angle, steer angle rate, and lateral deviation. The desired lateral deviation was always zero for the current time step (epoch).

A line trajectory was specified with a start point, an azimuth, and a length. In this case, all reference states were zero.

An arc trajectory was specified with a centre, start point, and interior angle. The arc radius, R_{arc}, determined the reference steer angle through the relationship,

$$\tan(\delta) = \frac{\ell}{\rho}. \tag{5}$$

The parameter ρ is the radius of curvature, and $R_{\text{arc}} = \rho$ for an arc. The reference yaw rate was calculated from equation (4). Since the radius of curvature in an arc was constant, reference steer angle was constant and hence reference steer angle rate was zero.

A spiral trajectory was specified with a centre, start point, interior angle, and 'width', denoted w. The spiral decreased or increased (depending on the sign of w) one width per revolution. Therefore, the spiral radius, R, as a function of the swept angle, θ, was $R = R_0 + \gamma\theta$ where $\gamma = w/2\pi$ and $R_0 = \|(x,y)_{\text{start}} - (x,y)_{\text{centre}}\|$. The spiral's radius of curvature was[5]

$$\rho = \frac{[R^2+\gamma^2]^{\frac{3}{2}}}{R^2+2\gamma^2}. \tag{6}$$

(Note that, unlike an arc, the radius of curvature at a particular point along the spiral did not equal the spiral radius.)

Reference steer angle was calculated using equations (5) and (6), and reference yaw rate came from equation (4). Reference steer angle rate was

$$\dot{\delta}_{\text{ref}} = \frac{1}{1+\left(\frac{\ell}{\rho}\right)^2}\left(-\frac{\ell}{\rho^2}\right)\dot{\rho}. \tag{7}$$

The time derivative of the spiral's radius of curvature, $\dot{\pi}$, equalled

$$\dot{\rho} = \frac{R\gamma\dot{\theta}\,(R^2+\gamma^2)^{\frac{1}{2}}(R^2+4\gamma^2)}{(2\gamma^2+R^2)^2}.$$

The time derivative of the swept angle, $\dot{\theta}$, equalled (using the curve length integral)[5]

$$\dot{\theta} = \frac{V}{\sqrt{(R^2+\gamma^2)}}. \tag{8}$$

A curve trajectory was specified only by a discrete series of points on the field. Two cubic splines, one in north and the other in east coordinates, fit the input points and were smoothed by a user-controlled fit parameter.[6] The splines parameters were defined by the Euclidean distance between the input points, denoted s.

The angle of the curve tangent in the inertial frame was

$$\psi_{\text{ref}} = \arctan\left(\frac{y'}{x'}\right). \tag{9}$$

The (′) operator denotes the derivative of the variable with respect to s. With curve length represented by m, the reference yaw rate was

$$\begin{aligned}\dot{\psi}_{\text{ref}} &= \frac{dm}{dt}\frac{ds}{dm}\frac{d\psi}{ds}\\ &= V\left[\frac{x'y''-x''y'}{(x'^2+y'^2)^{\frac{3}{2}}}\right].\end{aligned} \tag{10}$$

The local radius of curvature could have been computed and used to calculate reference steer angle as in equation (5); however, this solution was not as numerically stable because the radius of curvature approached infinity as sections along the curve approached a straight line. Instead, equations (4) and (10) were used to generate the reference steer angle. Reference steer angle rate was

$$\begin{aligned}\dot{\delta}_{\text{ref}} &= \frac{V\delta'}{\sqrt{(x'^2+y'^2)}}\\ &= V\ell\frac{\left[\begin{array}{c}(x'^2+y'^2)\,(x'y'''-x'''y')\\ -3(x'y''-x''y')\,(x'x''+y'y'')\end{array}\right]}{(x'^2+y'^2)^3+\ell^2(x'y''-x''y')^2}\end{aligned}$$

4. CLOSED-LOOP CONTROL. Linear controllers and estimators were designed[7] and scheduled on forward velocity. For lines, arcs, and spirals, a control law of the form

$$u_c = -K^T(\hat{x} - x_{\text{ref}}) \tag{11}$$

yielded satisfactory performance. However, this technique resulted in unsatisfactory performance for curved trajectories. Instead, linear-quadratic control with reference state tracking[8] was used for curves. Using the desired trajectory, future reference states were determined for N future epochs. These reference states were back-propagated from N epochs in the future back to the current epoch to generate a series of feed-forward control vectors, b_k, used in conjunction with the current state estimate, $\hat{x}_k$, to generate a control signal for every future epoch and, at the end of the back-propagation, the current epoch. Only the current epoch's control signal was actually used to control the tractor. This process was repeated at every epoch:

$$\begin{aligned}
S_{k+1} &= P_{k+1} + Q_{k+1} \\
P_k &= \Phi^T[S_{k+1} - S_{k+1}\,\Gamma(\Gamma^T S_{k+1}\,\Gamma + R)^{-1}\Gamma^T S_{k+1}]\Phi \\
K_k^T &= -[\Gamma^T S_{k+1}\,\Gamma + R]^{-1}\Gamma^T S_{k+1}\,\Phi \\
v_k &= -[\Gamma^T S_{k+1}\,\Gamma + R]^{-1}\Gamma^T[S_{k+1}\,\Phi\hat{x}_k + b_{k+1}] \\
b_k &= [\Phi^T + K_k\,\Gamma^T]\,b_{k+1} - Qx_{\text{ref},k}
\end{aligned}$$

Φ was the discretised state transition matrix, and Γ was the discretised control input vector. S and P were covariance matrices, and K was the control state vector. P and b initialised to zero. The design weighting matrices (Q and R) and the number of future epochs (N) were determined experimentally. If N was too low, the controller did not have enough information about the future to generate a control signal that accounted for changing reference conditions. If N was set too high, reference states far into the future had little impact on the current epoch's control signal. There was also a significant computational cost associated with increased N. Finally, future reference states were expressed in the current epoch's coordinate frame since the equations of motion were linearised about a straight line. Therefore, reference states far into the future might diverge into a non-linear region if the curve was changing rapidly.

5. TEST PLATFORM. A Deere and Co. 7800 tractor was outfitted with an array of four single-frequency GPS antennas and an equipment rack installed inside the cab. Mounted in the rack was a 90 MHz PC running the Lynx operating system. An Orthman electro-hydraulic valve actuated the front wheels, and a potentiometer measured front-wheel angle. Both the potentiometer and the actuator interfaced with the computer through a Motorola MC68HC11 microprocessor. Non-linearities in both the valve and the potentiometer were compensated for through the use of look-up tables. The positioning software used was a commercial version of the software used in the Integrity Beacon Landing System.[1] The system was manufactured by the IntegriNautics Corporation, a company recently founded by several Stanford Ph.Ds from this department who specialised in developing high-precision GPS techniques. Tractor position was

calculated at 5 Hz with IntegriNautics software using code and carrier phase measurements from a Trimble receiver. A Trimble TANS Vector produced attitude measurements at 10 Hz. The IntegriNautics positioning system used an IntegriNautics IN-200A pseudolite for initial integer-cycle ambiguity resolution.[9]

6. EXPERIMENTAL RESULTS. Data was collected at various speeds between 0·7 and 2·8 m/s without an implement attached to the tractor. Controller performance was judged on the basis of mean and standard deviation. Figure 2

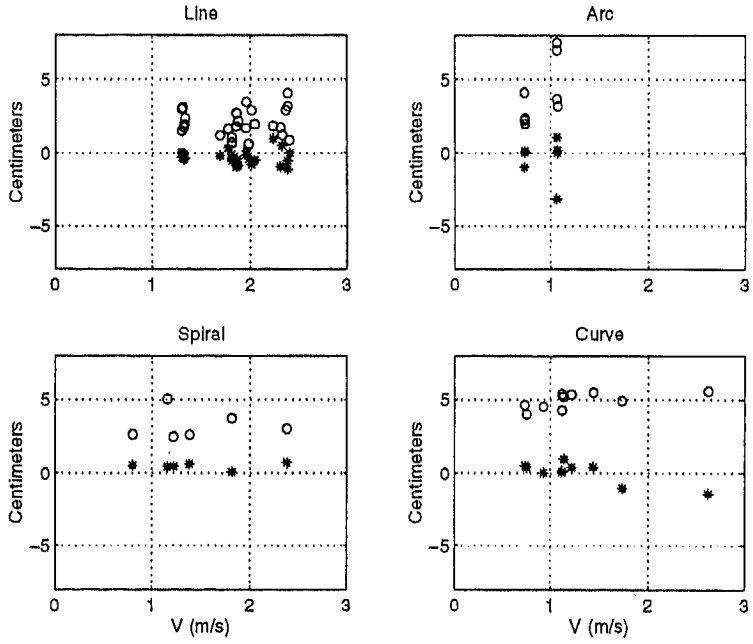

Fig. 2. Experimental data, no implement

shows mean ('*') and standard deviation ('o') as functions of velocity for all four of trajectories shown in Fig. 3. Ground disturbances had a strong effect on standard deviations.

A towed implement, a 'disker', was attached to the tractor and the experiment repeated at a new location (the original test site did not permit use of an implement). Though the new test site did not have enough room for arcs and spirals, both lines and curves were tested. Fig. 4 shows the lateral error mean and standard deviation. Although the standard deviations in lateral error did increase, the authors noted that most of that increase came from the stronger ground disturbances; the new test site was sloped at roll angles of up to 10 degrees, and the effect of small disturbances was more pronounced. The lack of integral control or bias estimation in the estimator accounts for the strong negative bias in the mean for both lines and curves. Either technique could have been used to zero out the bias.

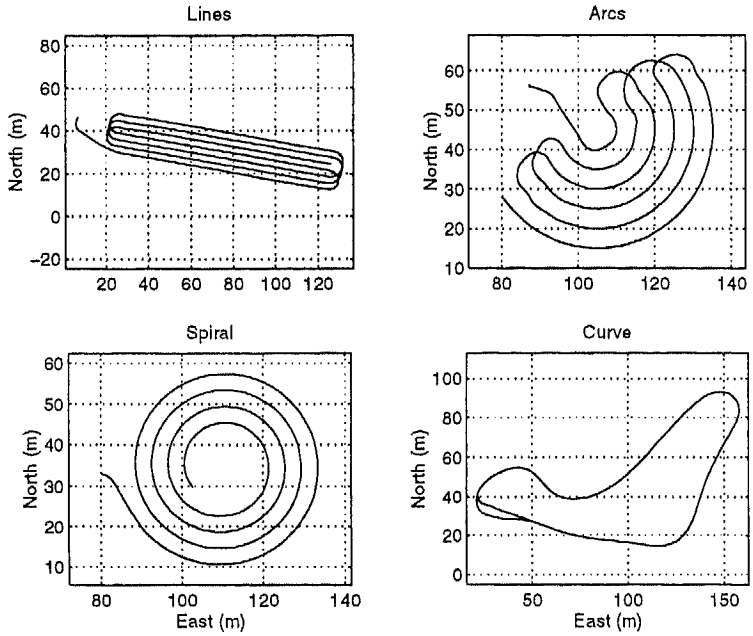

Fig. 3. Experimental trajectories

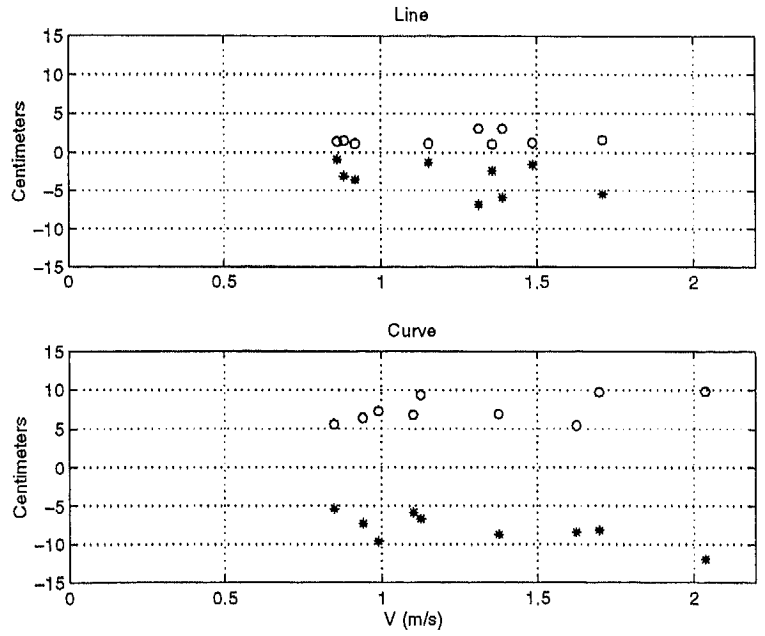

Fig. 4. Experimental data, towed implement

For curves, a linear controller which used only current reference state information (equation 11) was compared against the feed-forward control architecture mentioned previously. In Table 1, Controller 2 used the

TABLE 1. CURVE CONTROLLER COMPARISON

V (m/s)		Controller 1	Controller 2
0·75	mean (cm)	4·7	0·4
	1-σ (cm)	11·6	4·0
2·80	mean (cm)	8·3	−1·4
	1-σ (cm)	26·4	5·6

feed-forward control architecture while Controller 1 used only the current error information. Clearly, feed-forward control was a significant improvement over the control law used for the three other trajectory types. For comparison, an experienced human driver was asked to drive as straight a line in any speed and direction he chose without implement. Fitting a line to his trajectory revealed a standard deviation of 11·8 cm.[4]

7. CONCLUSION. Four basic trajectories were identified as building blocks for constructing useful reference trajectories for an automatically guided farm tractor. A realistic and simple model was detailed, and the reference trajectories were used to generate reference states. A control architecture that accounted for the changing reference information was implemented on a farm tractor and demonstrated 1 σ accuracy below 6 cm for all type of trajectories over a realistic velocity range without implement and less than 10 cm 1 σ with implement on sloped terrain.

ACKNOWLEDGEMENTS

This research was sponsored by Deere and Co. Any opinions, findings, conclusions, or recommendations expressed in this publication are those of the authors and do not necessarily reflect the views of Deere and Co.

REFERENCES

[1] Cohen, C. E. *et al.* (1995). Autolanding a 737 using GPS integrity beacons. *Navigation*, 42 (3): 467–486.

[2] Montgomery, P. (1996). *Carrier Differential GPS as a Sensor for Automatic Control*. PhD thesis, Stanford University.

[3] Cohen C. E., Pervan, B., Lawrence, D., Cobb, S., Powell, D. and Parkinson, B. W. (1994). Real-time flight testing using integrity beacons for GPS Category III precision landing. *Navigation*, 41 (2): 145–157.

[4] O'Connor, M. L. (1997). *Carrier-Phase Differential GPS for Automatic Control of Land Vehicles*. PhD thesis, Stanford University.

[5] Kreyszig, E. (1993). *Advanced Engineering Mathematics*. John Wiley & Sons, Inc., 7th edition.

[6] Späth, H. (1995). *One-Dimensional Spline Interpolation Algorithms*. A. K. Peters.

[7] Franklin, G. F., Powell, J. D. and Workman, M. (1990). *Digital Control of Dynamic Systems*. Addison-Wesley Publishing Co., Inc. 2nd edition.

[8] Anderson, B. D. O. and Moore, J. B. (1991). *Optimal Control, Linear Quadratic Methods*. Prentice-Hall, Inc., 1st edition.

[9] O'Connor, M. L., Bell, T., Elkian, G. and Parkinson, B. (1997). Real-time CDGPS initialization for land vehicles using a single pseudolite. In *Proceedings of ION National Technical Meeting*, pages 717–724. Institute of Navigation, Jan. 1997.

KEY WORDS

1. Automation. 2. Vehicle Control. 3. GPS.